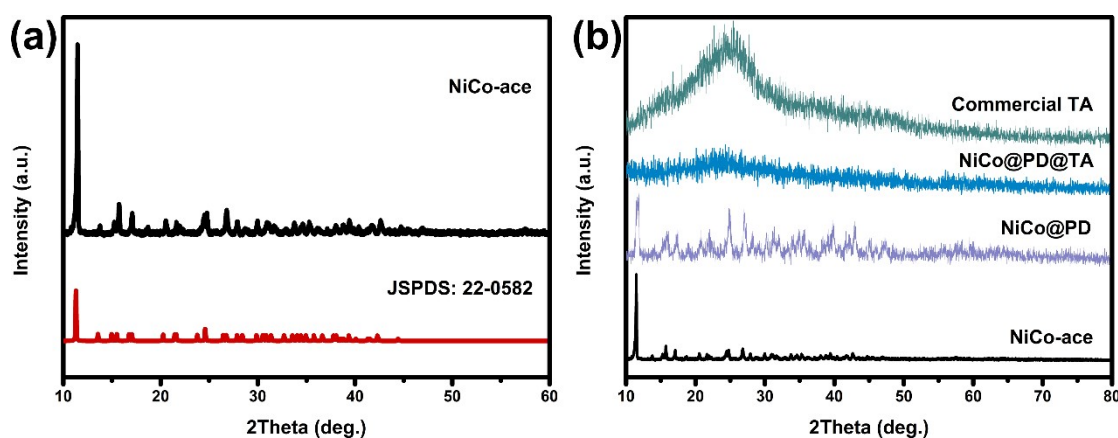


Interfaces engineering in NiSe<sub>2</sub>/Ni<sub>2</sub>Co/CoSe<sub>2</sub> heterostructures encapsulated in hollow carbon shell for high-rate Li-Se batteries

Yuqing Cao<sup>a</sup>, Feifei Lei<sup>a</sup>, Yunliang Li<sup>a</sup>, Yifang Fu<sup>a</sup>, Jun Zhao<sup>a</sup>, Shilun Qiu<sup>a</sup> and Zongtao Zhang<sup>a\*</sup>

<sup>a</sup> State Key Laboratory of Inorganic Synthesis and Preparative Chemistry, College of Chemistry, Jilin University, Changchun 130012, China.

\*Corresponding author. E-mail: [zzhang@jlu.edu.cn](mailto:zzhang@jlu.edu.cn) (Z. Zhang)



**Fig. S1** XRD patterns of (a) precursor NiCo-ace and (b) intermediate products NiCo-ace@PD and NiCo@PD@TA.

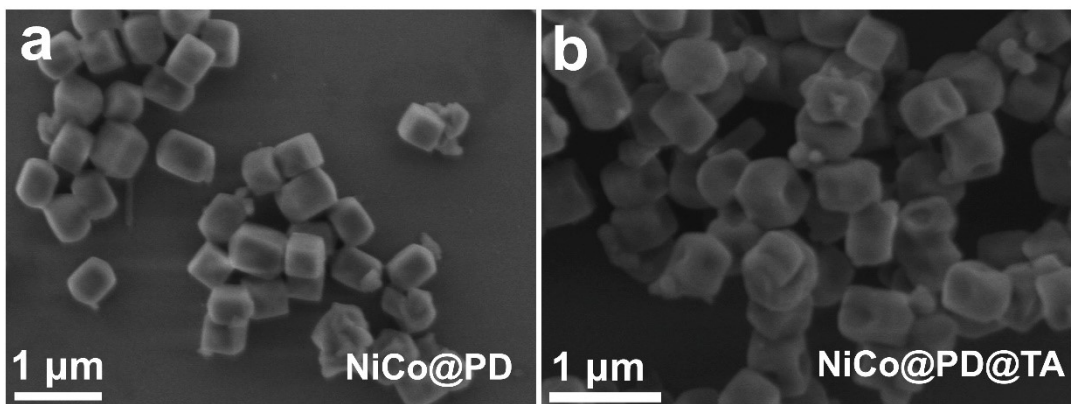


**Fig. S2** SEM images of intermediates (a) NiCo@PD and NiCo@PD@TA.

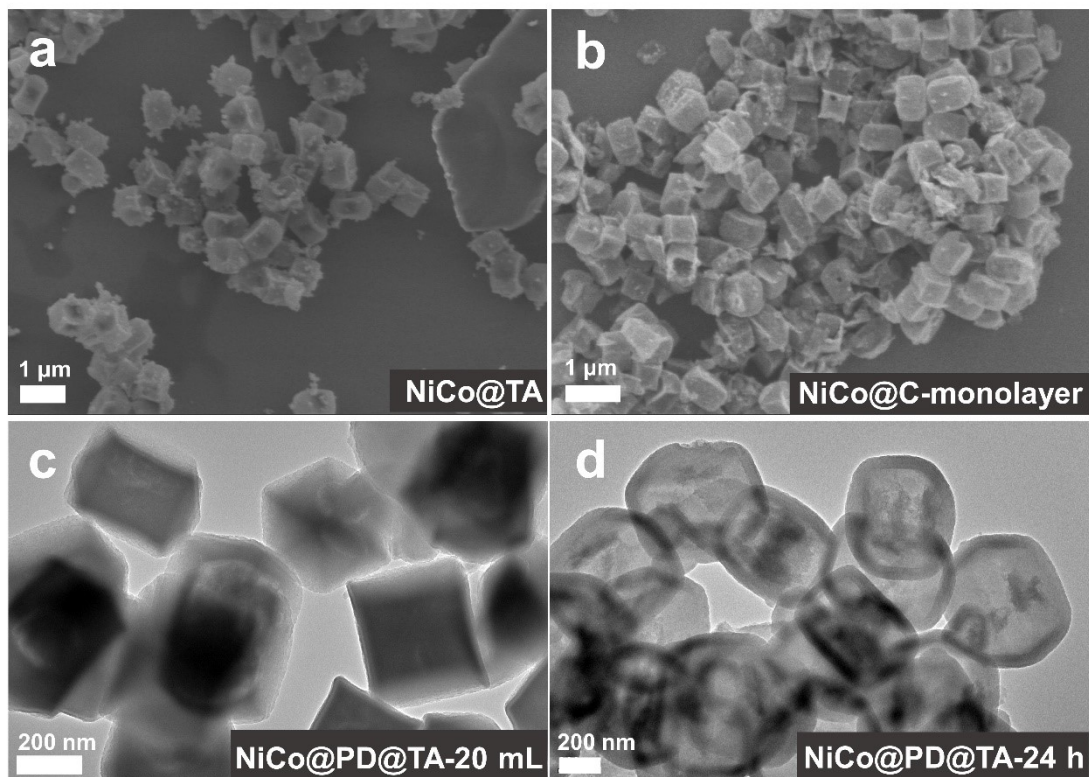


**Fig. S3** SEM images of contrast samples (a) NiCo@TA without PD layer and (b) corresponding carbonized product NiCo@C-monolayer, (c) NiCo@PD@TA-20 mL, (d) NiCo@PD@TA-24 h.

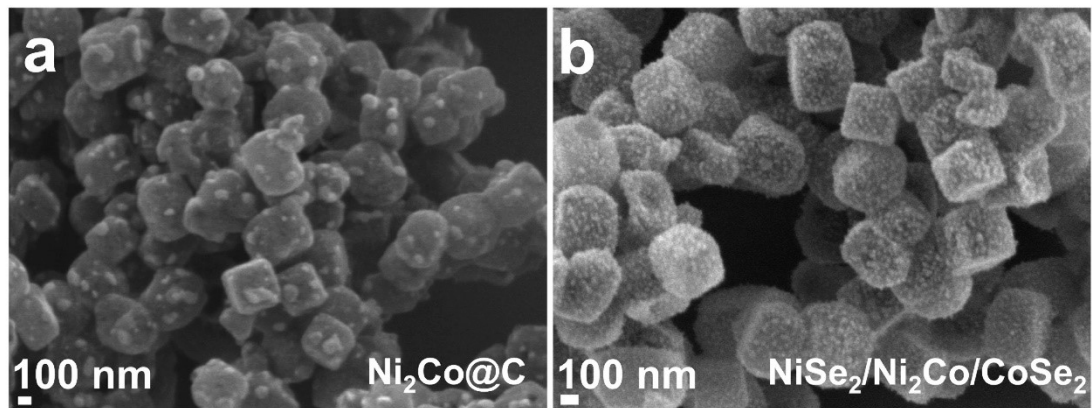


**Fig. S4** SEM images of (a)  $\text{Ni}_2\text{Co}@\text{C}$  and (b)  $\text{NiSe}_2/\text{Ni}_2\text{Co}/\text{CoSe}_2$ .

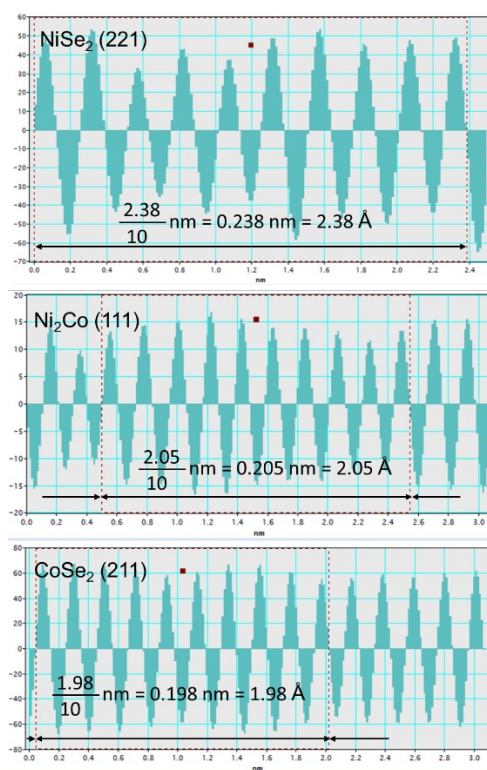


**Fig. S5** The profiles of corresponding intensity variations to determine crystal plane spacing in Figure 2c.

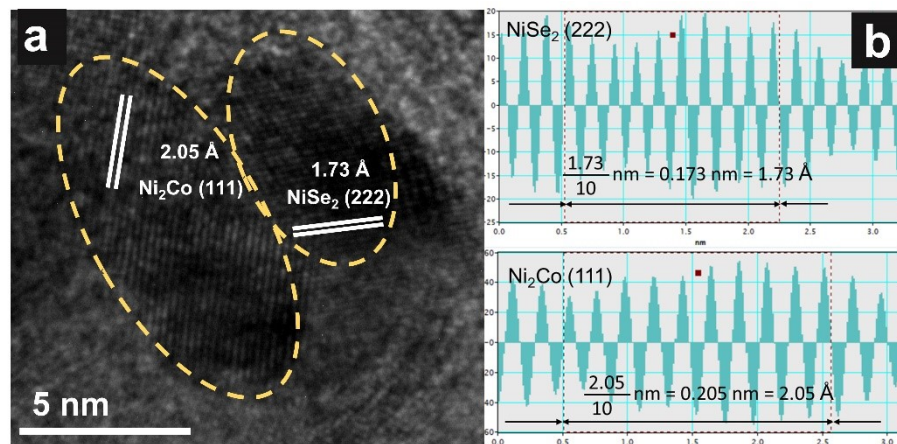


**Fig. S6** (a) The heterointerface of  $\text{Ni}_2\text{Co}$  and  $\text{NiSe}_2$  and (b) the profiles of corresponding intensity variations of crystal plane spacing.

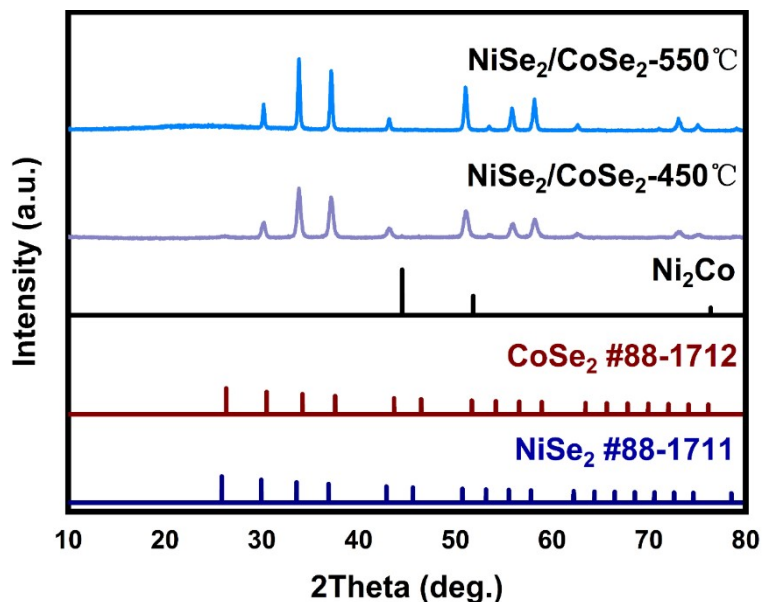


**Fig. S7** XRD patterns of contrast samples heterogenous  $\text{NiSe}_2/\text{CoSe}_2$ .

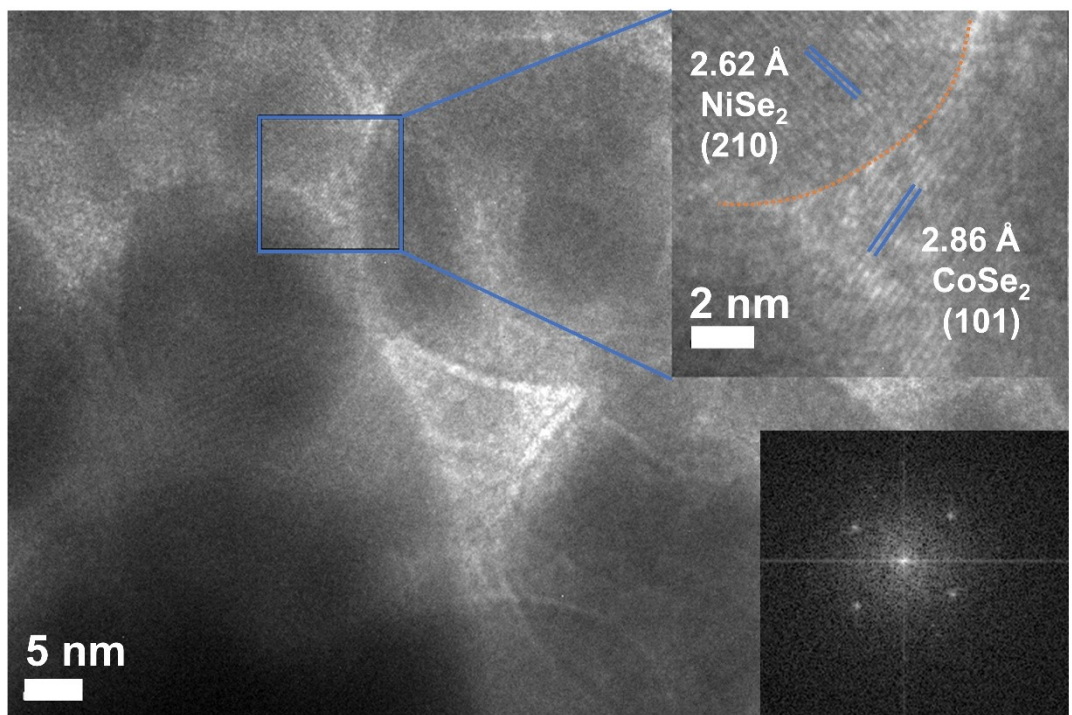


**Fig. S8** The HRTEM image of contrast sample  $\text{NiSe}_2/\text{CoSe}_2$  with single heterointerface.

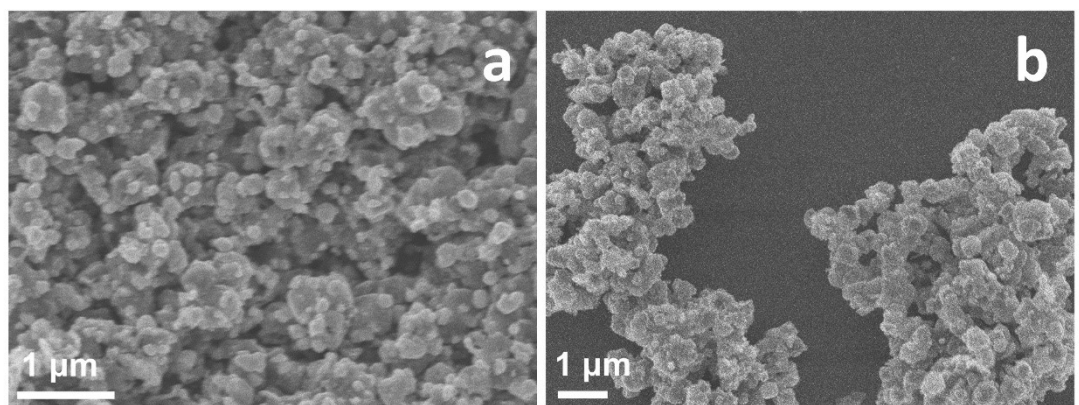


**Fig. S9** SEM images of (a)  $\text{NiSe}_2/\text{CoSe}_2@Se$  and (b)  $\text{NiSe}_2/\text{Ni}_2\text{Co}/\text{CoSe}_2@Se$ .

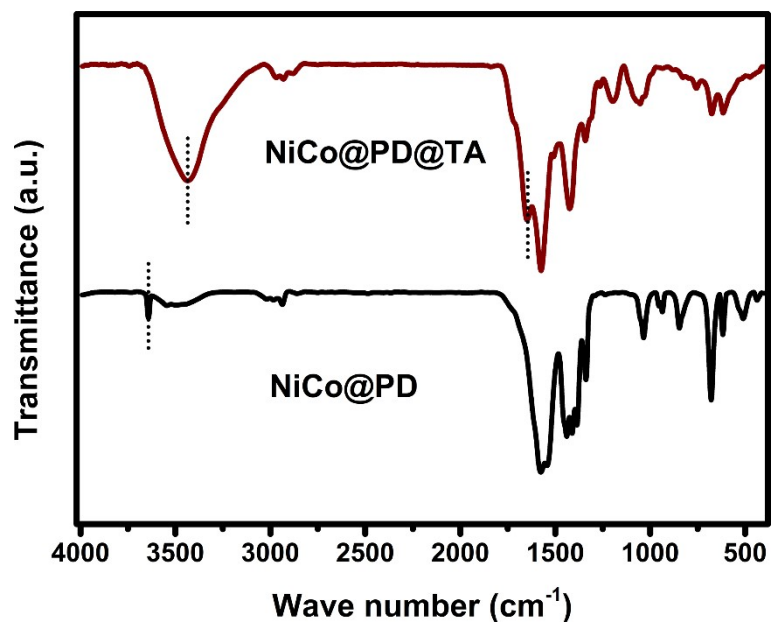


**Fig. S10** The FTIR spectra of intermediate products NiCo@PD and NiCo@PD@TA.

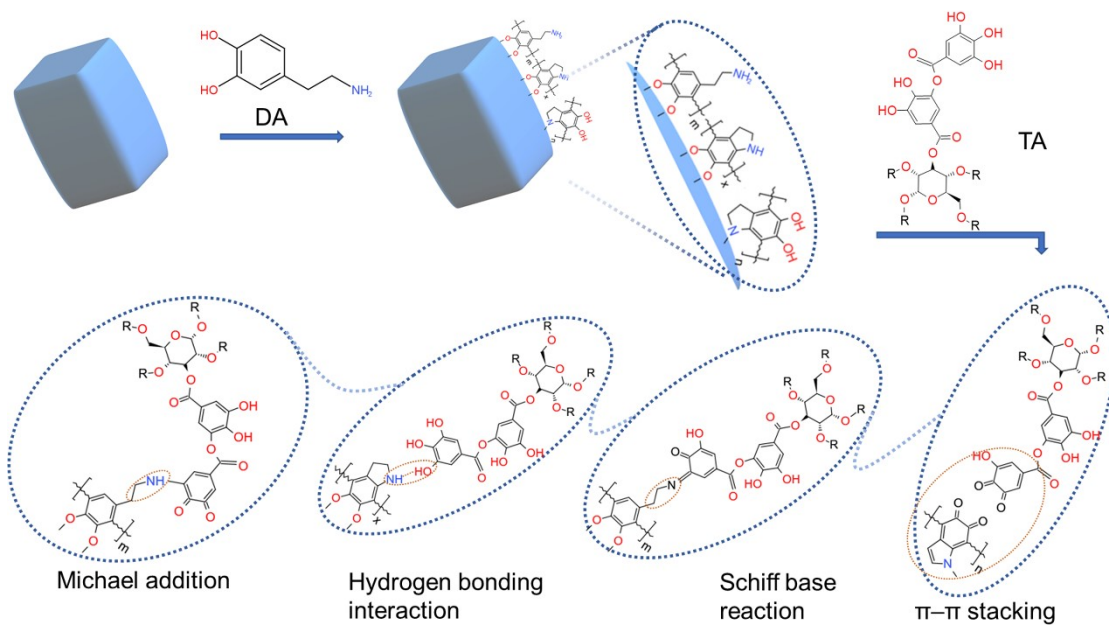


**Fig. S11** The schematic illustration of the linking process between PD layer and TA layer with four possible functional group reactions.

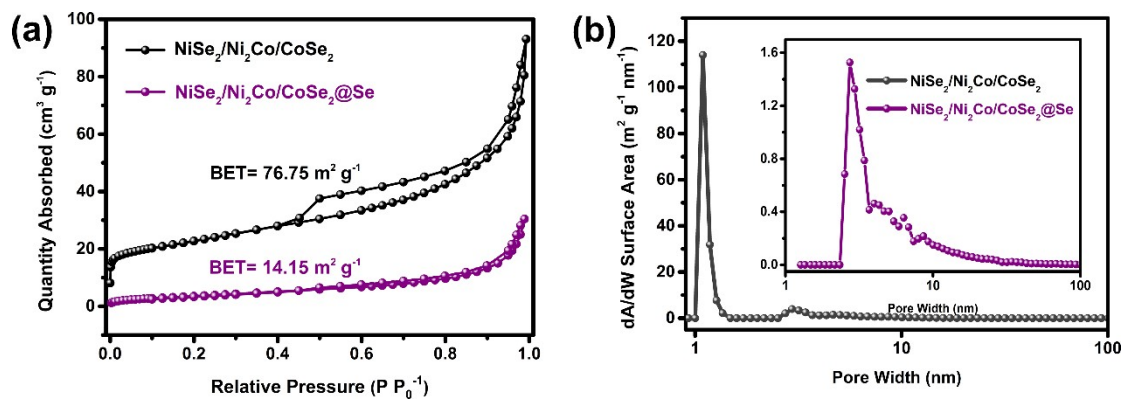


**Fig. S12** (a) The nitrogen adsorption–desorption isotherms and (b) the pore size distribution of  $\text{NiSe}_2/\text{Ni}_2\text{Co}/\text{CoSe}_2$  and  $\text{NiSe}_2/\text{Ni}_2\text{Co}/\text{CoSe}_2@\text{Se}$ .

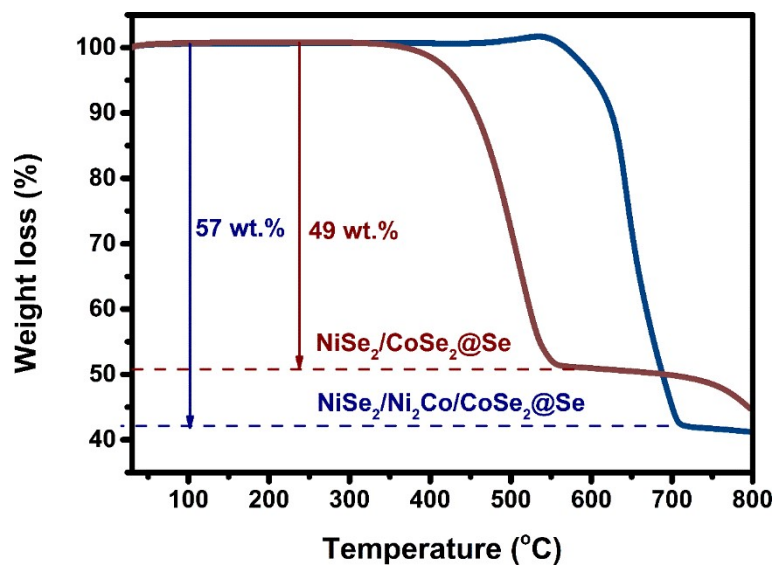


**Fig. S13** The TG curves of  $\text{NiSe}_2/\text{Ni}_2\text{Co}/\text{CoSe}_2@\text{Se}$  and  $\text{NiSe}_2/\text{CoSe}_2@\text{Se}$  in  $\text{N}_2$  atmosphere.

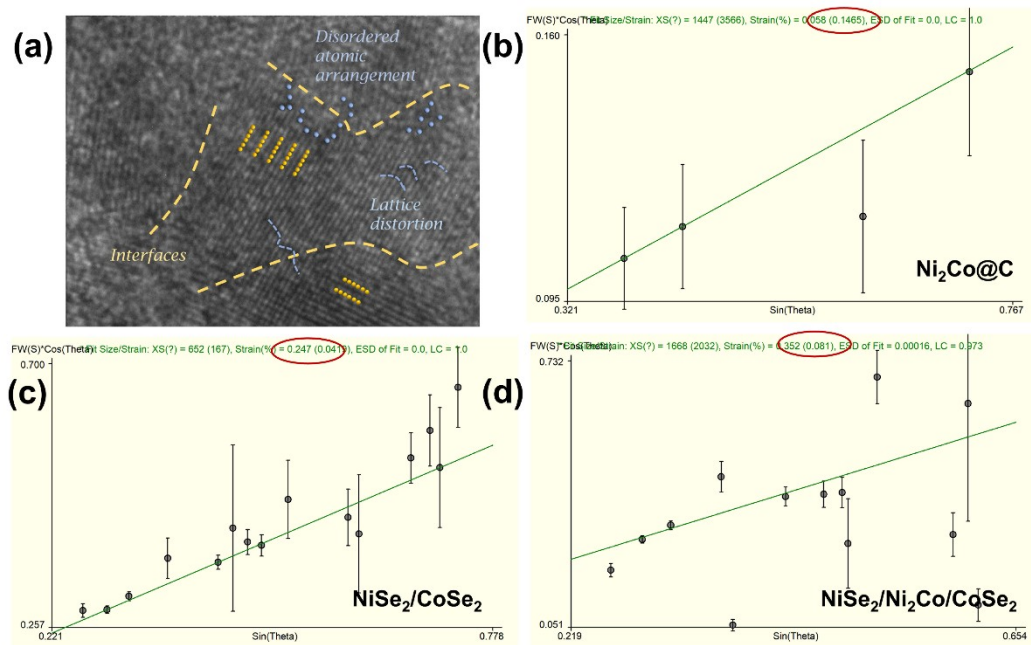


**Fig. S14** (a) The scheme of subtle distortion at heterointerfaces. (b-c) Size and strain plots of  $\text{Ni}_2\text{Co}@\text{C}$ ,  $\text{NiSe}_2/\text{CoSe}_2$  and  $\text{NiSe}_2/\text{Ni}_2\text{Co}/\text{CoSe}_2$  calculated by XRD Patterns in software MDI Jade 6.

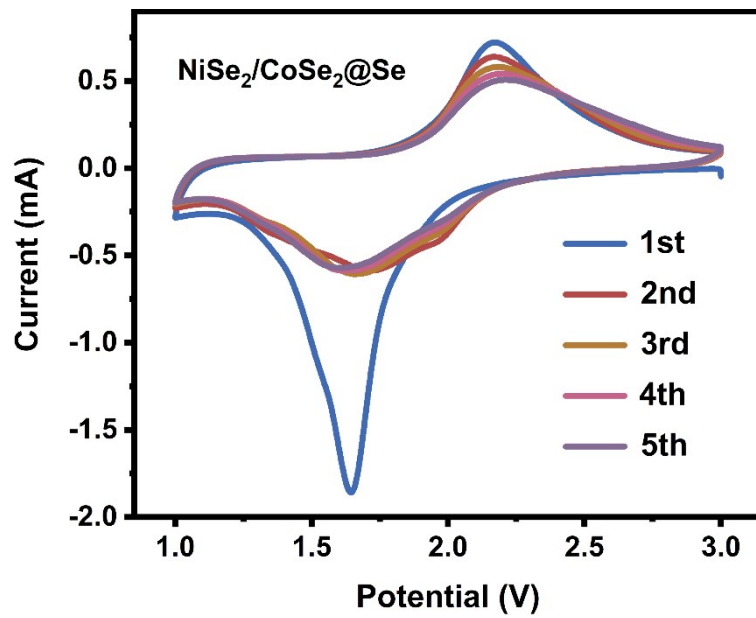


**Fig. S15** CV curves of  $\text{NiSe}_2/\text{CoSe}_2@\text{Se}$  cathode at  $0.2 \text{ mV s}^{-1}$  in Li-Se batteries.

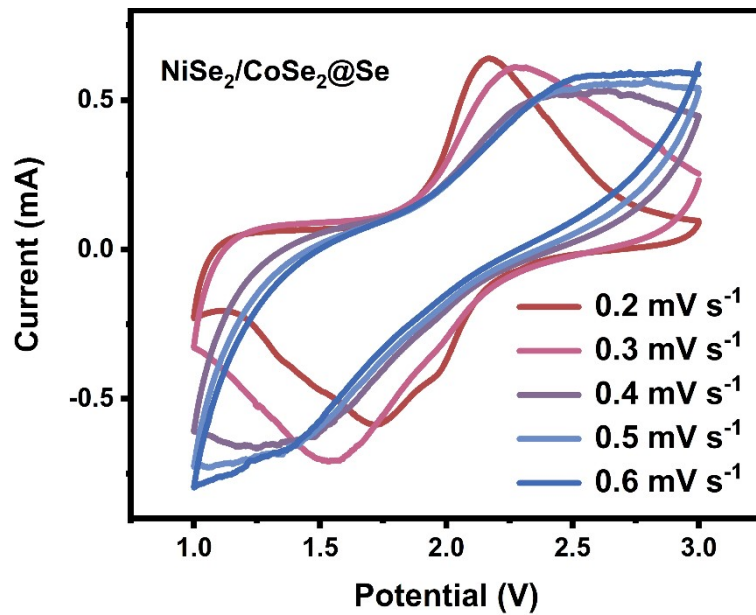


**Fig. S16** CV curves of  $\text{NiSe}_2/\text{CoSe}_2@\text{Se}$  cathode from  $0.2$  to  $0.6 \text{ mV s}^{-1}$  in Li-Se batteries.

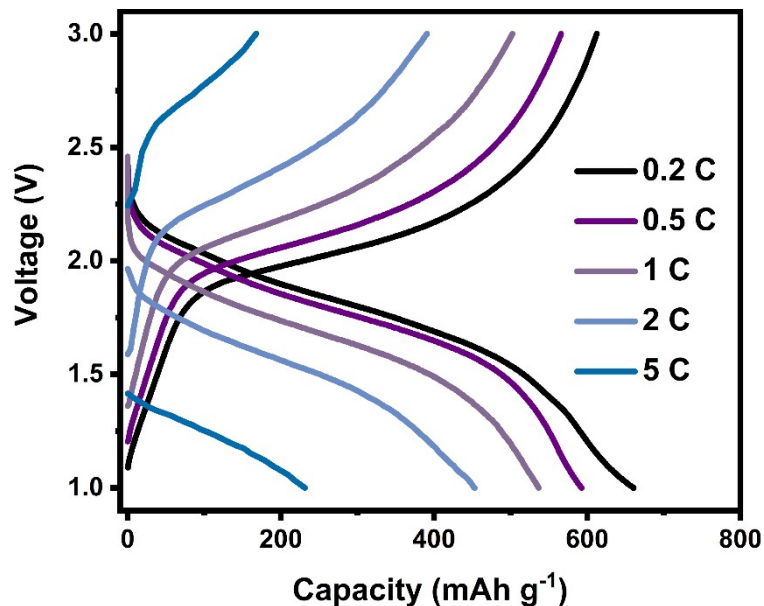


**Fig. S17** The galvanostatic charge-discharge curves at  $0.2 \text{ C}$  of  $\text{NiSe}_2/\text{Ni}_2\text{Co}/\text{CoSe}_2@\text{Se}$ .

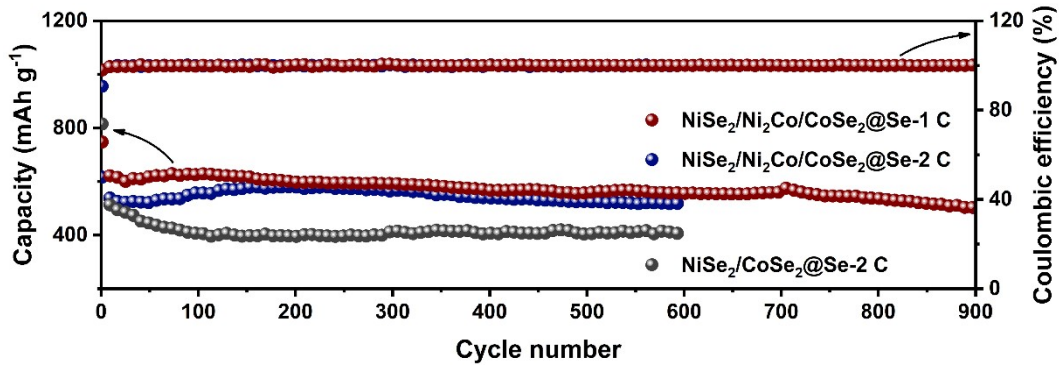


**Fig. S18** Cycling performance of  $\text{NiSe}_2/\text{Ni}_2\text{Co}/\text{CoSe}_2@\text{Se}$  and  $\text{NiSe}_2/\text{CoSe}_2@\text{Se}$  (Se loading: 0.9 mg cm<sup>-2</sup>).

**Table S1.** Comparison of electrochemical performances of  $\text{NiSe}_2/\text{Ni}_2\text{Co}/\text{CoSe}_2@\text{Se}$  with other carbonaceous hosts for Li-Se batteries reported in literatures.

Material	Current density (1C=675mA g <sup>-1</sup> )	Cycle number	Capacity (mAh g <sup>-1</sup> )
$\text{Se}@\text{CoSe}_2\text{-PC}^1$	1 C	100	408
$\text{Se}@\text{Co}_{\text{SA}}\text{-HC}^2$	5 C	1500	340
$\text{PANI}@\text{Se/C-G}^3$	2 C	500	528.6
A4-carbon/Se <sup>4</sup>	3 C	2000	343
HPC/Se <sup>5</sup>	2 C	800	451
NS-K-PC/Se <sup>6</sup>	1 C	500	394.2
$\text{Se}@\text{HHCS}^7$	10 C	2000	357
$\text{Se/CZIF-5}^8$	1 C	700	400
<b>This work</b>	<b>1 C</b>	<b>900</b>	<b>503</b>
	<b>2 C</b>	<b>600</b>	<b>515</b>
	<b>12 C</b>	<b>2200</b>	<b>324</b>

## References

1. H. Tian, H. Tian, S. Wang, S. Chen, F. Zhang, L. Song, H. Liu, J. Liu and G. Wang, *Nature communications*, 2020, **11**, 1-12.
2. X. Wang, Y. Tan, Z. Liu, Y. Fan, M. Li, H. A. Younus, J. Duan, H. Deng and S. Zhang, *Small*, 2020, **16**, 2000266.
3. J. Yang, H. Gao, D. Ma, J. Zou, Z. Lin, X. Kang and S. Chen, *Electrochimica Acta*, 2018, **264**, 341-349.
4. G. D. Park, J. H. Kim, J.-K. Lee and Y. C. Kang, *Journal of Materials Chemistry A*, 2018, **6**, 21410-21418.
5. L. Cheng, C. Ma, W. Lu, X. Wang, H. Yue, D. Zhang and Z. Xing, *Chemical Engineering Journal*, 2022, **433**, 133527.
6. Q. Xia, J. Hu, Q. Chen and L. Zhang, *J. Colloid Interface Sci.*, 2022, **610**, 643-652.
7. Y. Wang, H. Hao, S. Hwang, P. Liu, Y. Xu, J. A. Boscoboinik, D. Datta and D. Mitlin, *Journal of Materials Chemistry A*, 2021, **9**, 18582-18593.
8. M. H. Aboonaser Shiraz, E. Rehl, H. Kazemian and J. Liu, *Nanomaterials*, 2021, **11**, 1976.